

MC-EKRT: A 3-d Monte Carlo implementation of the EKRT initial state

Jussi Auvinen

University of Jyväskylä

in collaboration with

Mikko Kuha, Kari J. Eskola, Henry Hirvonen, Yuuka Kanakubo, and Harri Niemi

[arXiv:2406.17592](https://arxiv.org/abs/2406.17592) and [arXiv:2407.01338](https://arxiv.org/abs/2407.01338)

INT, Seattle
July 29, 2024



Centre of Excellence
in Quark Matter

Motivation

Goal: Perform relativistic hydrodynamics simulations of $A + A$ heavy ion collisions to determine QCD matter properties by comparing to LHC & RHIC data

⇒ Need a realistic description of the initial state

We would like to extract such description from perturbative QCD

EKRT framework

- E_T production in $p + p$ can be explained as a production of multiple independent few-GeV partons (aka minijets); diverges at $p_T \rightarrow 0$, need a cutoff $p_T \geq p_{T0}$
- In high-energy $A + A$, minijet multiplicity can be regulated dynamically
- Original EKRT idea: minijet production saturates at low p_T when higher order processes $3 \rightarrow 2$, $4 \rightarrow 2$, etc. become as important as $2 \rightarrow 2$
⇒ cutoff p_{T0} obtained from

$$N_{AA}(p_0, \sqrt{s_{NN}}, y \sim 0) \frac{\pi}{p_{T0}^2} \propto \pi R_A^2 \Rightarrow p_{\text{sat}} = p_{T0}(\sqrt{s_{NN}}, A)$$

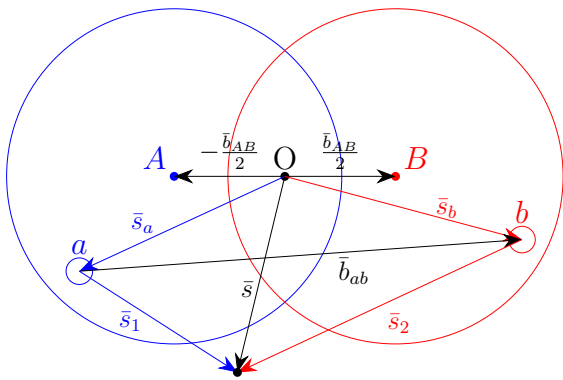
Why Monte Carlo?

- Extension to higher rapidities
- Energy and baryon number conservation
- Fluctuations in minijet production

Monte Carlo EKRT (MC-EKRT)

Triggering condition for $A + B$: for any nucleon pair $a \in A$ and $b \in B$,

$$|\bar{s}_b - \bar{s}_a| = |\bar{b}_{ab}| \leq \sqrt{\frac{\sigma_{\text{inel}}^{NN}(s_{NN})}{\pi}}.$$



MC-EKRT

Once the nuclear collision happens, we go through all nucleon-nucleon pairs $a + b$. The number of minijet pairs (dijets) produced in $a + b$ is sampled from the Poissonian probability

$$P_n^{ab}(\bar{b}_{ab}) = \frac{1}{n!} \left(T_{NN}(\bar{b}_{ab}) \sigma_{\text{jet}}^{ab} \right)^n e^{-T_{NN}(\bar{b}_{ab}) \sigma_{\text{jet}}^{ab}}$$

where σ_{jet}^{ab} is the inclusive minijet production cross section and $T_{NN}(\bar{b})$ is the convolution of the two Gaussian nucleon thickness functions $T_N(\bar{s})$ and thus also a Gaussian:

$$T_{NN}(\bar{b}_{ab}) = \frac{1}{4\pi\sigma_N^2} \exp\left(-\frac{|\bar{b}_{ab}|^2}{4\sigma_N^2}\right),$$

where the nucleon width parameter $\sigma_N(s_{NN})$ is extracted from the HERA J/ψ photo-production cross sections. The production point \bar{s} for each minijet candidate is then sampled from $T_N(\bar{s} - \bar{s}_a) T_N(\bar{s} - \bar{s}_b)$

The differential hard parton production cross section in leading order is

$$\frac{d\sigma_{\text{jet}}^{ab}}{dp_T^2 dy_1 dy_2} = \textcolor{red}{K} \sum_{ijkl} x_1 f_i^{a/A}(\{\bar{s}_a\}, x_1, Q^2) x_2 f_j^{b/B}(\{\bar{s}_b\}, x_2, Q^2) \frac{d\hat{\sigma}^{ij \rightarrow kl}}{dt}$$

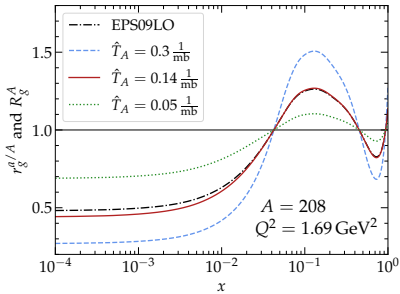
with the spatially dependent nPDF of the proton a in nucleus A defined as

$$f_i^{a/A}(\{\bar{s}_a\}, x, Q^2) \equiv r_i^{a/A}(\{\bar{s}_a\}, x, Q^2) f_i^p(x, Q^2)$$

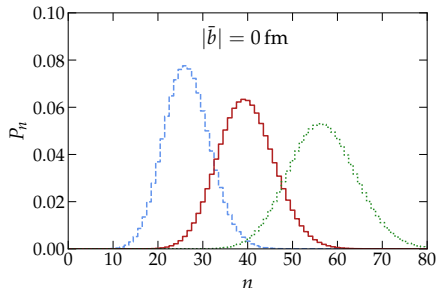
$$r_i^{a/A}(\{\bar{s}_a\}, x, Q^2) = \theta(c_A) \left[1 + \log(1 + c_A \hat{T}_A^a) \right] + \frac{\theta(-c_A)}{1 - c_A \hat{T}_A^a}$$

Here θ is the step function, $\hat{T}_A^a(\{\bar{s}_a\}) = \sum_{a' \neq a}^A T_{NN}(\bar{b}_{aa'})$ is the average overlap of nucleon a and nucleus A and $c_A(x, Q^2)$ is chosen so that the average over many nucleus configurations $\{A\}$ returns the global averaged nuclear modification:

$$R_i^A(x, Q^2) = \left\langle \frac{1}{A} \sum_a r_i^{a/A}(\{\bar{s}_a\}, x, Q^2) \right\rangle_{\{A\}}$$



Nuclear density effect on the snPDF
gluon modification



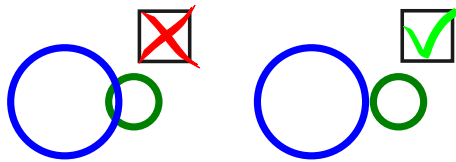
Nuclear density effect on the dijet
production probability

Minijet filtering

We define the minijet formation time as $\tau = \frac{1}{p_T}$, so the dijets with highest p_T are created first and the factorization is preserved; the later forming candidate dijets will be compared against the ones accepted earlier

The first filter to be applied is saturation: The candidate cannot be formed in the neighborhood of any earlier accepted dijet

$$|\bar{s}^{\text{cand}} - \bar{s}^{\text{acc}}| \not\leq \frac{1}{\kappa_{\text{sat}}} \left(\frac{1}{p_T^{\text{acc}}} + \frac{1}{p_T^{\text{cand}}} \right)$$



Minijet filtering

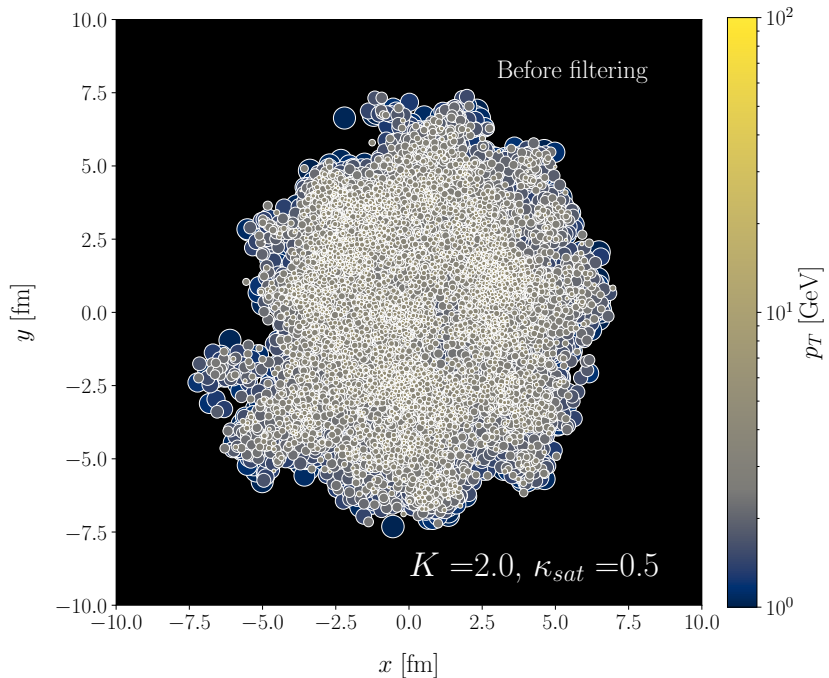
Nucleon-level filters (applied simultaneously, after the saturation filter):

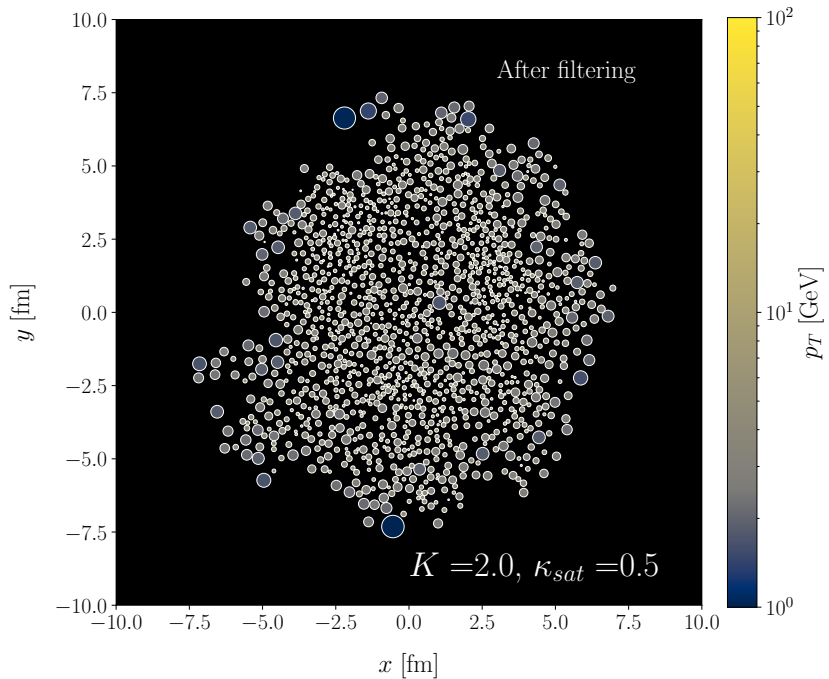
- Momentum conservation: The parent nucleons must have enough momentum left for the production of the candidate

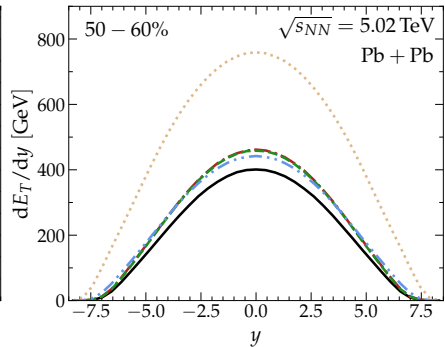
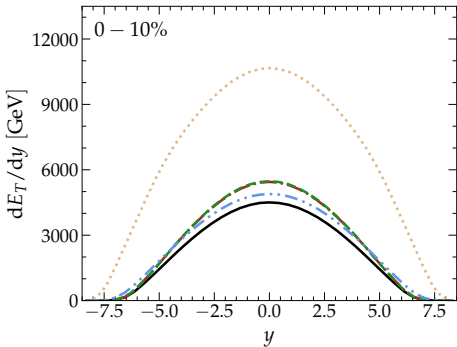
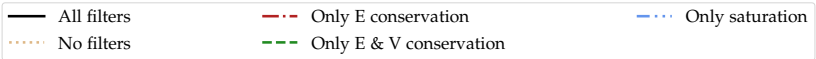
$$x_1 \leq 1 - \sum_{i=1}^n x_a^{(i)} \text{ and } x_2 \leq 1 - \sum_{j=1}^m x_b^{(j)}$$

where $x_a^{(i)}$ and $x_b^{(j)}$ represent the earlier subtracted momentum fractions from nucleons a and b , respectively

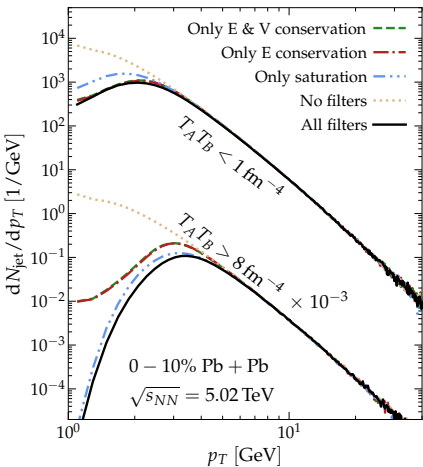
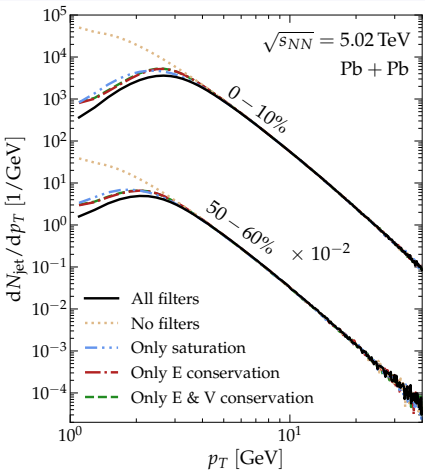
- Valence quark conservation: If the candidate minijet process involves a valence quark of a specific flavor from either of the parent nucleons, the nucleon must still have valence quarks of that flavor remaining







Dominant QCD mechanism: pQCD minijets + saturation



In all cases, the filter effects start at $p_T > 3 \text{ GeV}$ – well before the cutoff value $p_{T0} = 1 \text{ GeV}$

Energy density profile from minijets

Different minijets are formed at different times $\tau = \frac{1}{p_T}$, but we would like to start our hydro simulation at a constant proper time τ_{init}

⇒ Free stream all minijets to a common time $\tau_{\text{init}} \geq \tau_0 = \frac{1}{p_{T0}}$, (since minijet $p_T \geq p_{T0}$). In this study we use $\tau_{\text{init}} = \tau_0 = 0.2$ fm

For simplicity we set the longitudinal starting coordinate $z_0 = 0$ fm at $t = 0$ fm, so for any minijet i the rapidity coincides with the spacetime rapidity, $y_i = \eta_{s,i}$.

In hyperbolic coordinates the momentum 4-vector for minijet i at location (τ, η_s) is

$$p_i^\mu = (p_{T,i} \cosh(y_i - \eta_s), \bar{p}_{T,i}, \tau^{-1} p_{T,i} \sinh(y_i - \eta_s))$$

and the energy-momentum tensor component $T^{\alpha\beta}$ given by the minijets is

$$\begin{aligned} T^{\alpha\beta}(\tau, \bar{x}_\perp, \eta_s) &= \sum_i \int d^2 \bar{p}_T dy \frac{p^\alpha p^\beta}{p^\tau} \frac{1}{\tau} \cosh(y - \eta_s) \\ &\quad \cdot \delta^{(2)}(\bar{x}_\perp - \bar{x}_{\perp,i}) \delta(\eta_s - \eta_{s,i}) \delta^{(2)}(\bar{p}_T - \bar{p}_{T,i}) \delta(y - \eta_s) \end{aligned}$$

where $\delta(y - \eta_s)$ enforces the longitudinal scaling flow $y = \eta_s$.

Hydrodynamic simulations are run on a 3-d grid. However, simply depositing the energy of each minijet into a single cell would create too spiky initial profile, so we need a scheme to distribute the energy of a minijet over multiple cells

Similar to nucleons, here we represent each minijet i with a 3-d Gaussian distribution

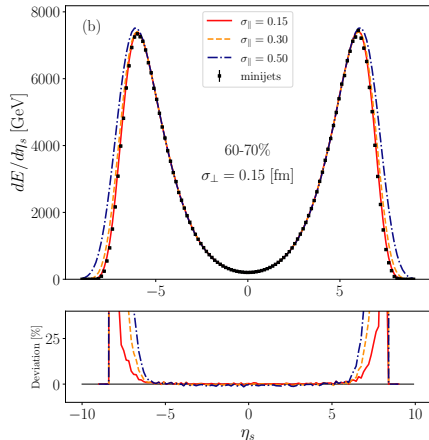
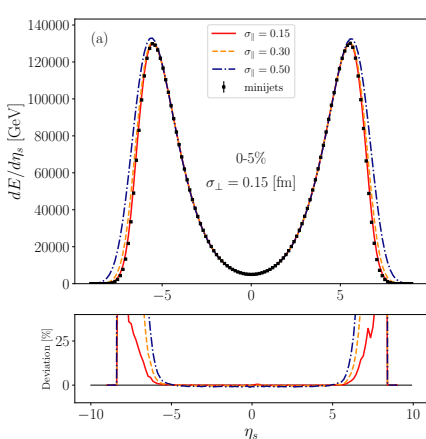
$$g_i(\bar{x}_\perp, \eta_s; \sigma_\perp, \sigma_\parallel) = \frac{1}{N} \exp\left(-\frac{1}{2} \frac{(\bar{x}_\perp - \bar{x}_{\perp,i})^2}{\sigma_\perp^2}\right) \exp\left(-\frac{1}{2} \frac{(\eta_s - \eta_{s,i})^2}{\sigma_\parallel^2}\right)$$

where the normalization factor N is the sum of the weights g_i over the hydro cells.

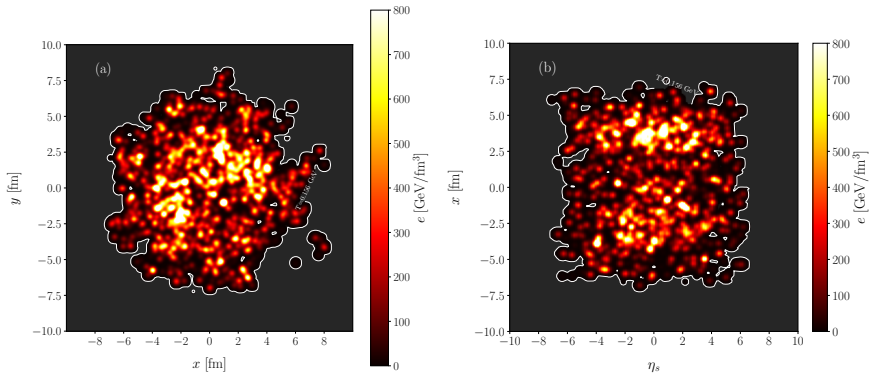
We can now replace the spatial delta functions $\delta^{(2)}(\bar{x}_\perp - \bar{x}_{\perp,i})\delta(\eta_s - \eta_{s,i})$ with $g_i(\bar{x}_\perp, \eta_s; \sigma_\perp, \sigma_\parallel)$ in the expression for $T^{\alpha\beta}$.

In these first proof-of-principle studies, we use an event-averaged initial state and hence keep only the $T^{\tau\tau}$ component of the energy-momentum tensor:

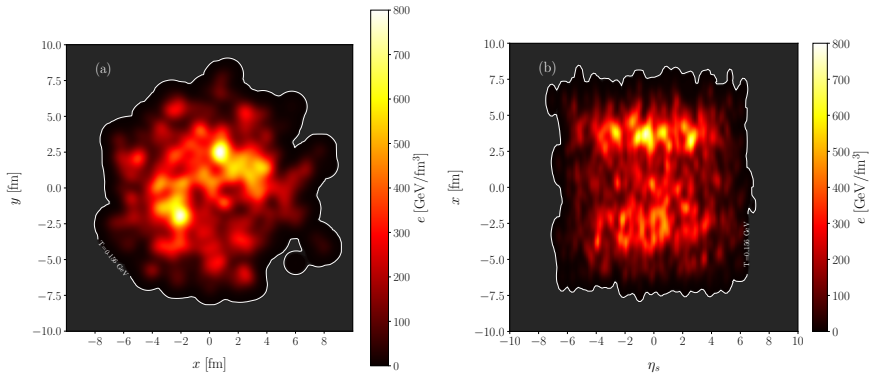
$$e(\tau, \bar{x}_\perp, \eta_s) \equiv T^{\tau\tau}(\tau, \bar{x}_\perp, \eta_s) = \frac{1}{\tau} \sum_i p_{T,i} g_i(\bar{x}_\perp, \eta_s; \sigma_\perp, \sigma_\parallel)$$



Single Pb+Pb 5 TeV event, $\sigma_{\perp} = 0.15$ fm, $\sigma_{\parallel} = 0.15$



Single Pb+Pb 5 TeV event, $\sigma_{\perp} = 0.40$ fm, $\sigma_{\parallel} = 0.15$



Event-averaged initial profile

We run the full (3+1)-d hydrodynamics simulations for one average profile per centrality class. The averaging procedure is as follows:

- Calculate energy density e for each event as described before
- For each event, convert energy density to entropy density using the equation of state
- Average over the e -by- e entropy densities
- Convert the average entropy density back to energy density

This procedure preserves the centrality dependence of e -by- e simulations as closely as possible

(3+1)-d hydrodynamics

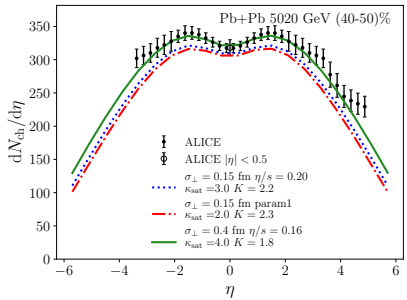
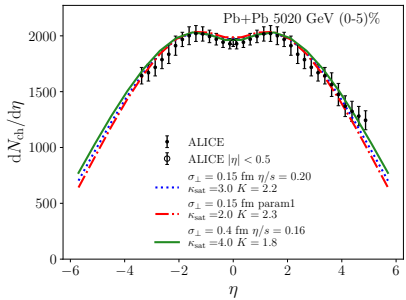
E. Molnar, H. Holopainen, P. Huovinen and H. Niemi, PRC **90**, 044904 (2014)

$$\partial_\mu T^{\mu\nu} = 0$$

$$T^{\mu\nu} = eu^\mu u^\nu - P(g^{\mu\nu} - u^\mu u^\nu) + \pi^{\mu\nu}$$

- Initial e from minijets, no initial transverse velocity or shear viscosity
- During the hydro evolution, the shear viscosity coefficient over entropy density is either constant $\eta/s = 0.16$ or 0.20 , or temperature dependent ([param1](#) from arxiv:1505.02677)
- No bulk viscosity
- Equation of state: $s95p$ -PCE-v1: partial chemical equilibrium with chemical freeze-out at $T_{\text{chem}} = 150$ MeV
P. Huovinen and P. Petreczky, NPA **837**, 26 (2010)
- Kinetic freezeout at $T_{\text{kin}} = 130$ MeV

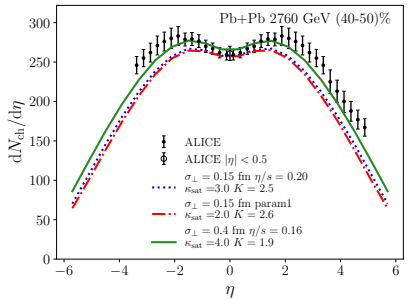
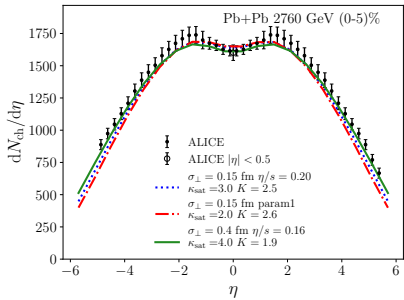
Charged particle multiplicity vs pseudorapidity



ALICE N_{ch} pseudorapidity data at 5 TeV from arxiv:1612.08966

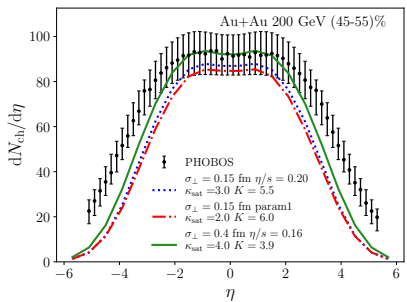
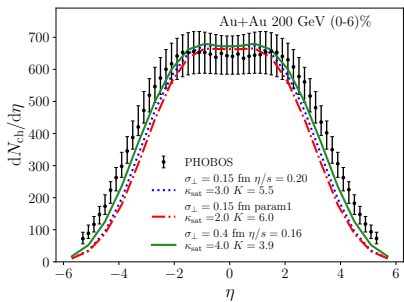
ALICE N_{ch} $|\eta| < 0.5$ data at 5 TeV from arxiv:1512.06104

Charged particle multiplicity vs pseudorapidity



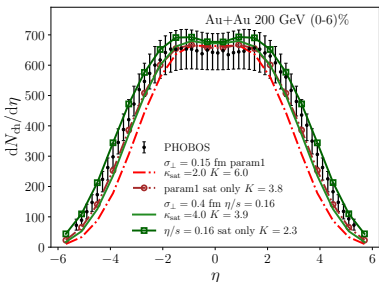
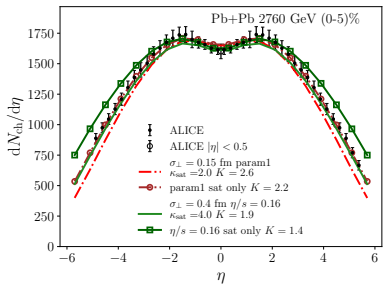
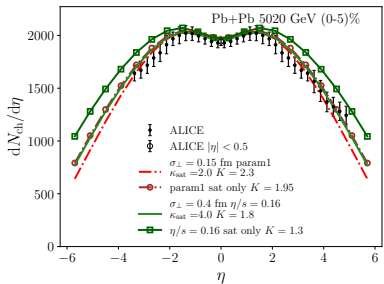
ALICE N_{ch} pseudorapidity data at 2.76 TeV from arxiv:1304.0347 and arxiv:1509.07299
ALICE N_{ch} $|\eta| < 0.5$ data at 2.76 TeV from arxiv:1012.1657

Charged particle multiplicity vs pseudorapidity

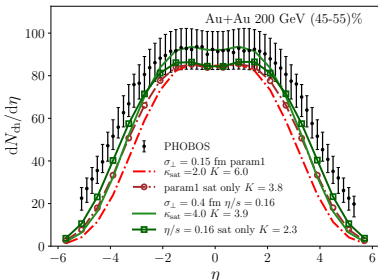
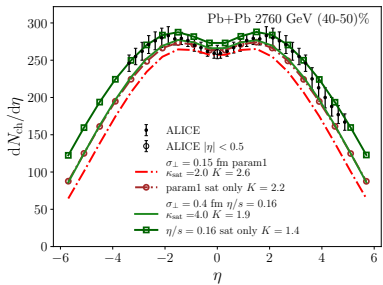
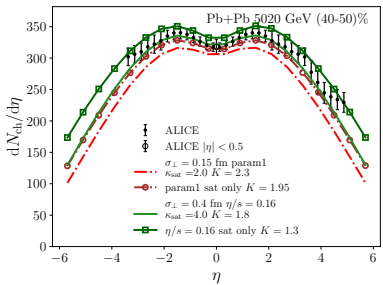


PHOBOS N_{ch} pseudorapidity data at 200 GeV from arxiv:nucl-ex/0210015

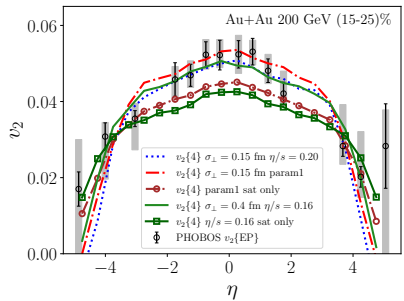
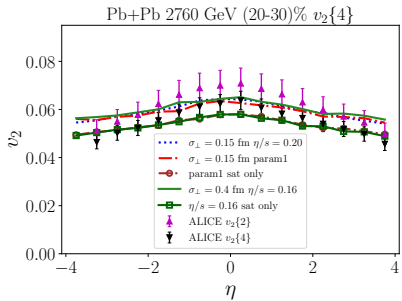
Effect of nucleon-level conservation laws



Effect of nucleon-level conservation laws



Charged particle v_2 vs pseudorapidity



ALICE data from arXiv:1605.02035

PHOBOS data from arxiv:nucl-ex/0407012

E-by-E simulations with nucleon substructure

Nucleon thickness function with N_h hotspots (we'll use $N_h = 3$):

$$T_N(\bar{s}) = \frac{1}{N_h} \sum_{i=1}^{N_h} \frac{1}{2\pi\sigma_h^2} \exp\left(-\frac{|\bar{s} - \bar{s}_i^h|^2}{2\sigma_h^2}\right)$$

where the hotspot locations \bar{s}^h are sampled from a 2-d Gaussian with a width $\sigma_s \Rightarrow$ total nucleon width $\sigma_N^2 = \sigma_s^2 + \sigma_h^2$

The triggering condition for $A + B$ collision is now based on minimum distance d_{\min}^{HS} between a hotspot in A and a hotspot in B :

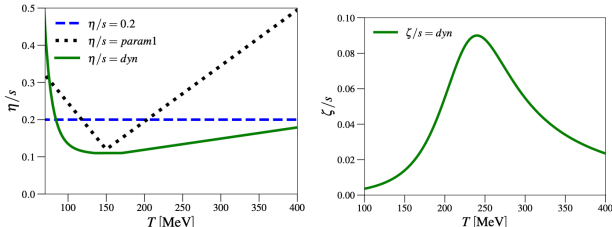
$$d_{\min}^{\text{HS}} < \sqrt{\frac{\sigma_{\text{HS}}}{\pi}}$$

where the effective hotspot cross section σ_{HS} is tuned to reproduce the same nucleus-nucleus cross section as the hotspot-less case with $\sigma_{\text{inel}}^{NN}$.

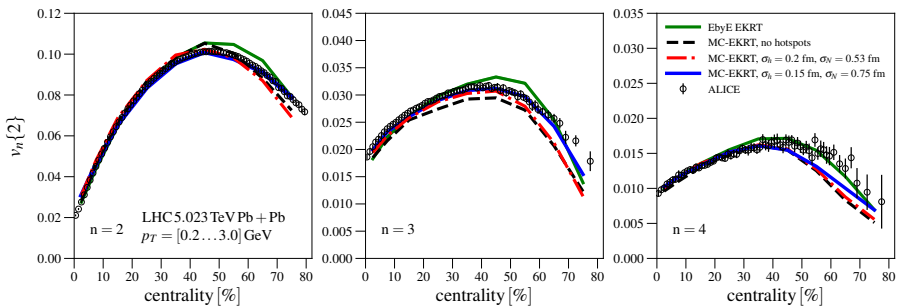
E-by-E simulations with nucleon substructure

The final observables are obtained using neural networks [arXiv:2303.04517] trained on a (2+1)-d fluid dynamics model [arXiv:2206.15207]

- Boost-invariant \Rightarrow Initialize with midrapidity minijets
 $\delta(\eta_s - \eta_{s,i}) \rightarrow \theta(\Delta y/2 - |\eta_{s,i}|)/\Delta y$; here $\Delta y = 1.0$
- Dynamical freezeout conditions $\tau_\pi \theta = C_{Kn}$ and $\gamma \tau_\pi / R = C_R$, where system size $R = \sqrt{\frac{A}{\pi}}$ is defined by the area A in which $Kn < C_{Kn}$
- Equation of state s95p-PCE-v1 with $T_{\text{chem}} = 155$ MeV
- Temperature-dependent shear and bulk viscous coefficients $(\eta/s)(T)$ and $(\zeta/s)(T)$

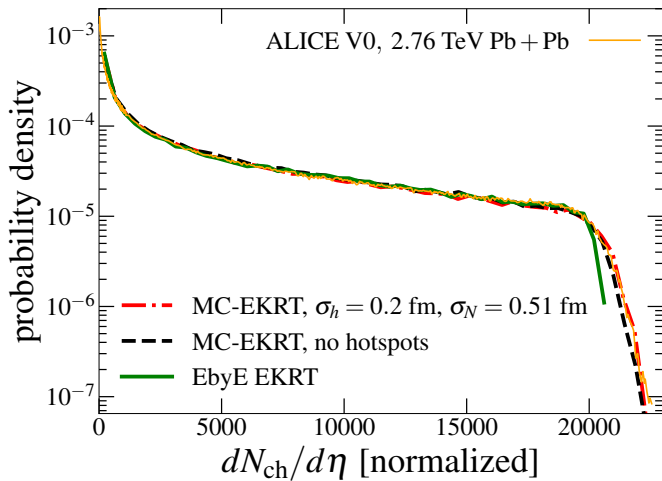


$v_n\{2\}$ at 5 TeV Pb+Pb collisions



ALICE data from arXiv:1804.02944

N_{ch} distribution at 2.76 TeV Pb+Pb collisions



ALICE data from arXiv:1301.4361

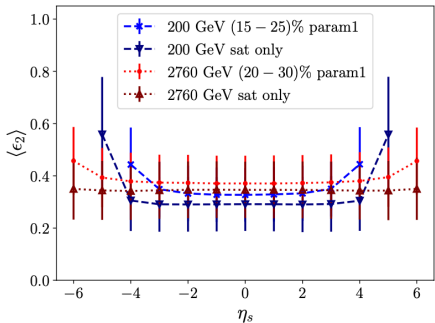
Summary: The novel event generator MC-EKRT

- pQCD minijet production + saturation, with corrections from nucleon-level momentum and valence quark conservation
- Extends the EKRT model to longitudinal dimension
- Novel EbyE-fluctuating snPDFs developed
- Main control parameters: pQCD K -factor ($\sqrt{s_{NN}}$ -dependent) and saturation strength κ_{sat} ($\sqrt{s_{NN}}$ -independent)
- Gaussian smearing and nucleon substructure introduce additional parameters: σ_{\perp} , σ_{\parallel} , σ_h , and σ_N
- The earlier good agreement of EKRT with data extends to larger rapidities
- Nucleon substructure improves the v_3/v_2 ratio, as well as the EbyE multiplicity distribution in the most central collisions

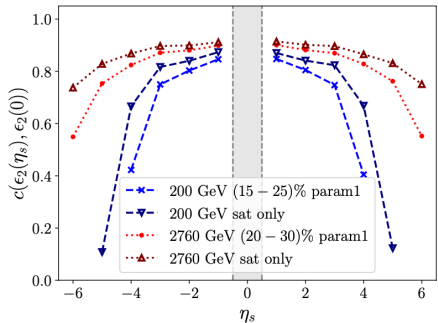
Backup slides

Spacetime rapidity dependence of eccentricity

From 3d-hydro runs before event-averaging



EbyE mean and standard deviation



Correlation to midrapidity